LUND UNIVERSITY

Theoretical EXAFS studies of a model of the oxygen-evolving complex of photosystem II obtained with the quantum cluster approach

Li, Xichen; Sproviero, Eduardo M.; Ryde, Ulf; Batista, Victor S.; Chen, Guangju

Link to publication

Total number of authors:
5

Theoretical EXAFS Studies of a Model of the Oxygen-Evolving Complex of Photosystem II Obtained with the Quantum Cluster Approach

Xichen Li[1,2,*], Eduardo M Sproviero[4], Ulf Ryde[3], Victor S Batista[4], Guangju Chen[1]

[1] College of Chemistry, Beijing Normal University, 100875, Beijing, China. [2] Department of Physics, ALBA NOVA, and Department of Biochemistry and Biophysics, Arrhenius Laboratory, Stockholm University, SE-106 91 Stockholm, Sweden. [3] Department of Theoretical Chemistry, Lund University, Chemical Center, P.O. Box 124, S-221 00 Lund, Sweden. [4] Department of Chemistry, Yale University, PO Box 208107, New Haven, CT 06520-8107, USA.

Correspondence to: Xichen Li (E-mail: *xli@fysik.su.se*)

ABSTRACT

The oxygen-evolving complex (OEC) of photosystem II is the only natural system that can form O_2 from water and sunlight and it consists of a Mn_4Ca cluster. In a series of publications, Siegbahn has developed a model of the OEC with the quantum mechanical (QM) cluster approach that is compatible with available crystal structures, able to form O_2 with a reasonable energetic barrier, and has a significantly lower energy than alternative models. In this investigation, we present a method to restrain a QM geometry optimization towards experimental polarized EXAFS data. With this method, we show that the cluster model is compatible with the EXAFS data and we obtain a refined cluster model that is an optimum compromise between QM and polarized EXAFS data.

KEYWORDS: Density functional calculations, Photosynthesis, Oxygen-evolving complex, Manganese, EXAFS spectroscopy.

INTRODUCTION

In nature, photosystem II (PSII) is the only system capable of forming O_2 from water and sunlight. The oxygen-evolving complex (OEC) located at the lumenal side of the thylakoid membrane of chloroplasts contains a Mn_4Ca cluster that catalyzes the key step of O–O bond formation in the photosynthetic process.

To elucidate the water oxidation mechanism, extensive studies have been carried out to determine the geometric structure of the OEC. In the past few years, breakthroughs in X-ray diffraction (XRD) have considerably clarified this issue,[1-4] suggesting a Mn_3Ca cuboidal core with the fourth manganese ion situated outside the cube (Figure 1a). However, it has been suggested that the XRD structures of the OEC are strongly affected by photoreduction and therefore not representative. Instead, alternative topologically motifs have been suggested,[5-7] based on polarized extended X-ray absorption fine structure (polarized EXAFS) studies of PSII single crystals, but it has been difficult to fit these motifs into the XRD framework of PSII.[8]
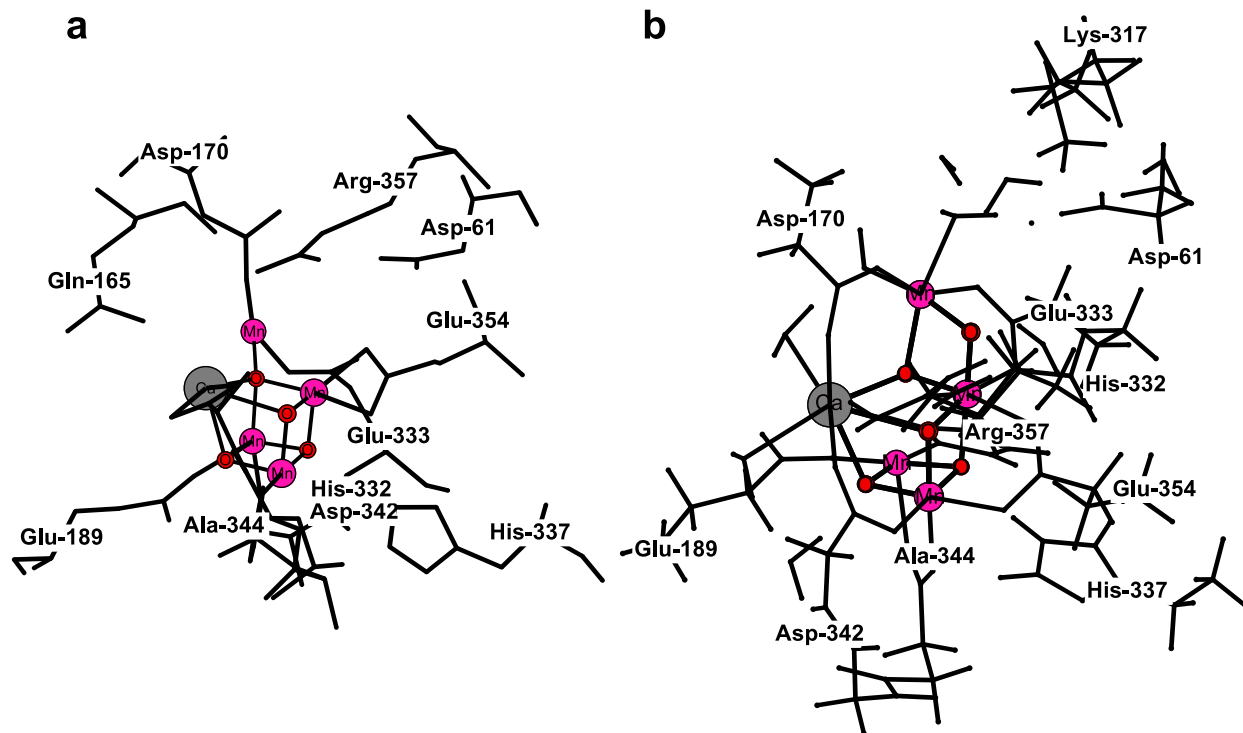
FIGURE 1. The 1.9 Å XRD structure[4] (a) and the cluster model[17] (b) of the OEC. The OEC core is shown with balls and sticks and the ligands with sticks for clarity. The figures were prepared using XYZViewer.

Parallel to the experimental structural work, significant progress has been made theoretically. Combined quantum mechanics and molecular mechanics (QM/MM) models have been developed from the XRD models,[9,11] assuming a minimum displacement of the metal cluster and ligating residues from their crystallographic positions after completing the coordination spheres of the metals by hydration. The resulting QM/MM models of the OEC have also been further refined based on the available high-resolution polarized EXAFS data, using a simple harmonic restraint towards the QM/MM structure in the EXAFS fit[10,11] In parallel, quantum mechanical (QM) optimizations of the isolated Mn_4Ca cluster with the aim of obtaining minimum energy structures and a reasonable activation energy for the formation of the O–O bond have suggested a structure (hereafter termed the cluster model), that initially was topologically quite different from the structures suggested by polarized EXAFS or by low-resolution XRD structures.[12-17] However, this topology was recently confirmed by the 1.9 Å XRD structure of the OEC[4] – only a minor change of the binding pattern of Asp-170 was needed to make the cluster model fully compatible with the 1.9 Å XRD model.[17]

In this article, we develop a method to combine QM geometry optimizations and a fit to the polarized EXAFS data, based on similar approaches for isotropic EXAFS data. We employ this method to the cluster model of the OEC, thereby, obtaining a structure that is an ideal compromise between the QM and EXAFS data, showing that the cluster model is compatible both with the XRD and polarized EXAFS data.[18,19]

METHODOLOGY

Instead of merely using the proposed Mn–Mn distances as discrimination criteria, techniques have been developed to utilize the polarized EXAFS spectra directly in the QM geometry optimization. In the present approach, a standard QM geometry optimization is performed in which the QM gradients are enhanced by EXAFS pseudo-gradients. The latter are obtained by numerical differentiation of the EXAFS χ^2 "goodness-of-fit" parameter for each intermediate structure.[18-19] Thereby, the final structure (called the refined cluster model below) will be an optimal compromise between the QM and the polarized EXAFS spectra.

Polarized EXAFS fit

We used the program FEFF 8.3[20-21] to calculate the theoretical polarized EXAFS scattering amplitudes and phase shifts. All polarized EXAFS fits were performed with IFEFFIT 1.2.11c.[22] Sample input files were kindly provided Junko Yano.[5] In essence, all possible paths with up to eight scattering legs (NLEG = 8) and a default path half-length value (RPATH) were considered, and the Debye–Waller parameters was fixed at 0.002 Å^{-2} in the calculations. Paths with χ and curved-wave amplitudes less than 4 and 2.5%, respectively, of that of the largest path (CRITERIA) were neglected.

Coordinates for FEFF calculations were obtained by transforming one monomer of PSII crystal from *Thermosynechococcus elongatus* (PDB: 1S5L) into all the eight polarized-EXAFS-active OEC sites by a combination of the local C_2 axis rotation and $P2_12_12_1$ space group transformations. Polarized EXAFS spectra in *k*-space were then directly calculated by FEFF (POLARIZATION keyword). The energy axis was converted into the momentum (*k*) space by using E_0 = 6543.3 eV.[10,11] A window function w(*k*), defined as a fractional cosine-square window (Hanning) with *k* = 1, was applied to the k^3-weighted EXAFS data. The windowed spectra obtained for a grid of *k*-points, equally spaced at 0.05 Å^{-1} in the 3.5–11.5 Å^{-1} *k*-range, were then Fourier transformed (FT) with a factor of 0.85 to obtain the FT-amplitudes in the reduced distance *R* space. The calculated and experimental EXAFS spectra were compared in the *R* range 1.0–4.5 Å.

Structural refinement based on polarized-EXAFS simulations

We have developed a technique to utilize the high-resolution polarized EXAFS data as restraints in a quantum mechanical (QM) geometry optimization. The approach is partly based on our previous QM/isotropic-EXAFS refinement procedure,[18-19] and it is analogous to the use of molecular mechanics (or QM)[23-24] to supplement the experimental data in crystallographic and NMR structure refinement.[25-26] Except in the most accurate crystal and NMR structures, there is not enough information in the experimental data to determine the positions of all atoms in the structure. Therefore, computational chemistry is used to ensure that the structure (bond lengths and angles) is chemically reasonable, and the result is a structure that is an optimum compromise between the experimental and computational data.

This is accomplished by defining an energy function

$$E_{\text{pEXAFS/QM}} = w_{\text{pEXAFS}}E_{\text{pEXAFS}} + E_{\text{QM}}$$

where E_{QM} is the standard QM energy and E_{pEXAFS} is an EXAFS pseudo-energy describing how well the current model (coordinates of all atoms) fit the polarized EXAFS data. The QM energies were obtained with Turbomole 6.1 using the Becke–Perdew-86 (BP86) density functional and the def2-SV(P) basis set for all the atoms.[27-33] The calculations involved the 196 atoms in Figure 1b. Following the original cluster calculations,[17] all atoms in the CH_3 or CH_2 groups that are used to truncate the cluster model were kept fixed during the geometry optimization. For the EXAFS pseudo-energy, there are several "goodness-of-fit" parameters and we have quite arbitrarily selected the sum of the χ^2 estimate along the three crystal axes, *a*, *b*, and *c*. These two energies have different units (E_{QM} is in energy units, e.g. kJ/mole, whereas E_{pEXAFS} is unit-less). Therefore, the two terms need to be weighted by the term w_{pEXAFS}, which determines the relative importance of the EXAFS and QM data. Considering the typical accuracy of the two methods (±0.02 Å for metal–ligand bond lengths in EXAFS and ±0.06 Å for the QM optimized structures),[34-36] w_{pEXAFS} is increased until χ^2 no longer changes.

The energy function in Eqn. (1) is then used in a standard QM geometry optimization, in which the forces are calculated by differentiation of this equation. The polarized EXAFS forces were obtained by numerical differentiation (with a step length 10^{-6} Å)[18] for the four Mn ions, the Ca ion, the bridging oxo atoms, and all the first-sphere ligating atoms along all three Cartesian directions.

The philosophy behind the QM/polarized-EXAFS method is that QM should provide the general structure of the complex and EXAFS provides the detailed metal–ligand and metal–metal bond lengths (correcting small errors in the QM calculations). The QM/polarized-EXAFS procedure is available from the authors upon request. Further information on the use of the program can be found in http://www.teokem.lu.se/~ulf/Methods/comqum_pe.html.

RESULTS AND DISCUSSION

Refinement

Figure 2 compares the polarized EXAFS spectra calculated from the original cluster model[17] and the refined cluster model with the experimental data. It can be seen that although the original cluster model does not match the experimental spectra satisfactorily, the refined cluster model reproduces the experimental data qualitatively along all three axes of the PSII crystal (the consistency is also clear from the low EXAFS χ^2 value, 45, as can be seen in Table 1).
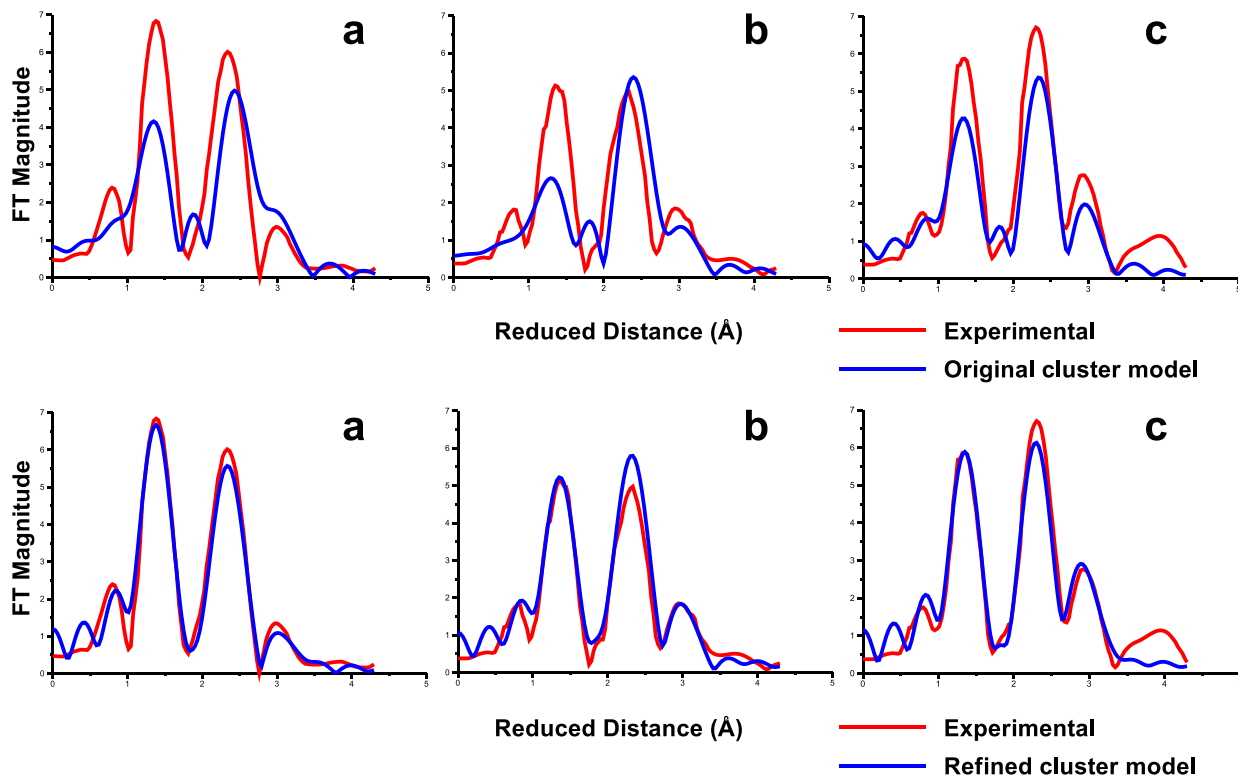
FIGURE 2 Comparison of the experimental polarized EXAFS spectra (red) and the calculated spectra (blue), along the PSII crystal axes *a*, *b*, and *c*, for the original cluster model (top panel), and the refined cluster model (bottom panel). The corresponding spectra in *k* space are given in the supplementary material (Figure S1).

TABLE 1 EXAFS χ^2 for refined structures and QM energy differences (kcal/mol) relative to the energy of the corresponding structure freely optimized with QM.

Structure	EXAFS χ^2	QM energy differences
Freely optimized with QM	384.0	0.0
Refined	45.4	11.6
Refined, Mn2–Mn3=3.2 Å	60.7	22.8

Figure 3 shows an overlay of the original[17] and the refined cluster models. It can be seen that the two models are essentially identical, showing that it is possible to accurately reproduce the polarized EXAFS spectra using the topology of the cluster model. For the metal–oxo core and the first-sphere ligating atoms, the structural changes induced by the refinement are small and within the expected errors in the DFT calculations (Figure 3).[37] For example, all Mn–Mn and Mn–Ca distances decrease by up to 0.10 and 0.13 Å. There are also differences of up to 0.12 Å for the Mn–O distances.

Still, these small differences for a large number of distances sum up to a QM energy difference between the original and the refined structure of 11.6 kcal/mol (Table 1). This energy difference was obtained by fixing the Cartesian coordinates of the four Mn ions, the Ca ion, the bridging oxo atoms, and the other first-sphere ligating atoms at their positions after the EXAFS refinement, and performing a new geometry optimization without any EXAFS restraints. It should be emphasized that this energy difference is the EXAFS restraint to the QM optimized structure (i.e. mainly a correction of systematic errors in the QM method) and is therefore not significant for discriminating between different structures, which should be done at the same theoretical level.[16] The refined cluster structure is a slight improvement of the original cluster model, removing systematic errors in the DFT method by the restraints to the EXAFS data. It also shows that the cluster model is in accordance with the polarized EXAFS data and that possible photoreduction of the XRD structure does not have a major influence on the structure.

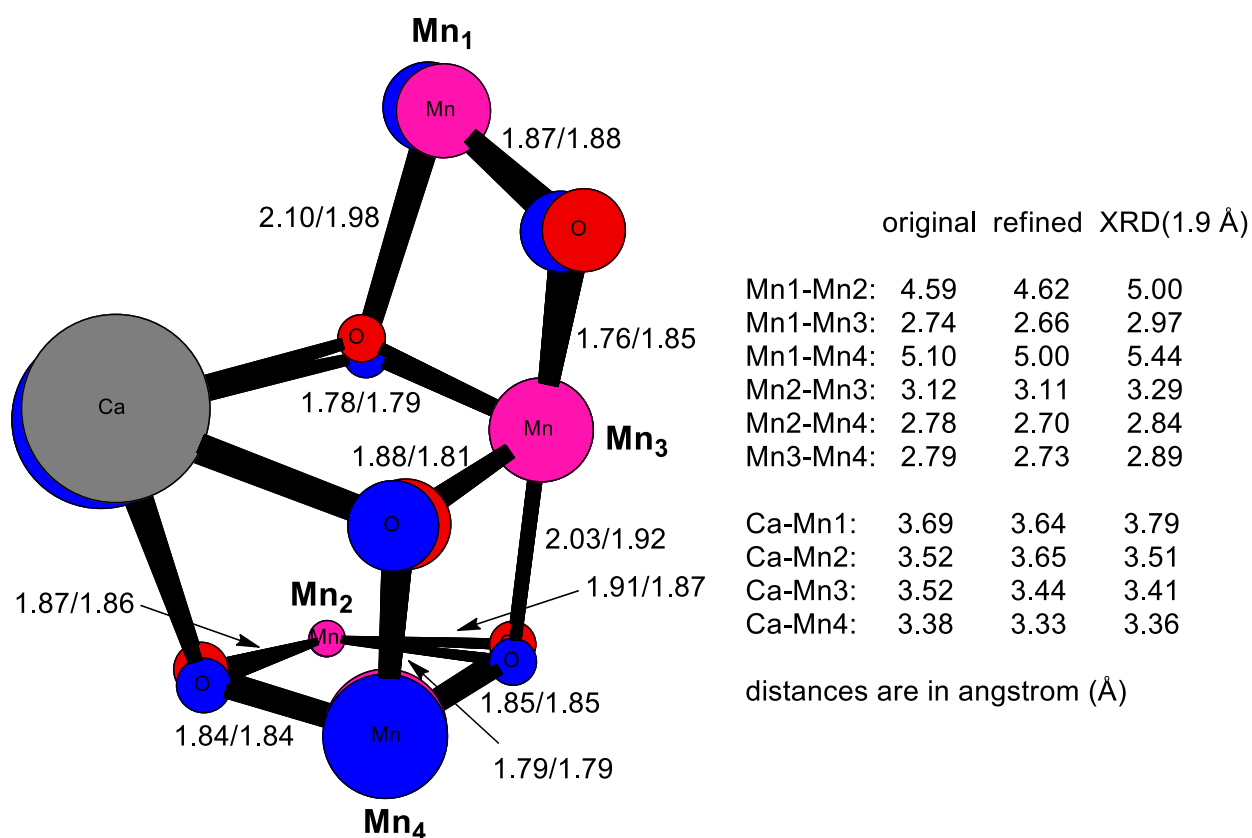|	original	refined	XRD(1.9 Å)
Mn1-Mn2:	4.59	4.62	5.00
Mn1-Mn3:	2.74	2.66	2.97
Mn1-Mn4:	5.10	5.00	5.44
Mn2-Mn3:	3.12	3.11	3.29
Mn2-Mn4:	2.78	2.70	2.84
Mn3-Mn4:	2.79	2.73	2.89
Ca-Mn1:	3.69	3.64	3.79
Ca-Mn2:	3.52	3.65	3.51
Ca-Mn3:	3.52	3.44	3.41
Ca-Mn4:	3.38	3.33	3.36

distances are in angstrom (Å)

FIGURE 3. Overlay of the original cluster model (blue) and the refined cluster model of the OEC in PSII. Only the OEC core is shown for clarity. The Mn–O bond lengths are shown in the model (values before the slash are for the original cluster model), whereas the Ca–Mn, and Mn–Mn distances are shown to the right (also for the 1.9 Å XRD structure[4]).

We have analyzed the contributions of various scatters for the polarized EXAFS spectra (Figure S2). The general features of the spectra are well reproduced by the Mn_4CaO_5 core, but the finer details, especially at $R' > 2.5$ Å, require the inclusion of the other first-shell ligating atoms. The analysis of various atomic contributions is supplemented by a path analysis for each Mn ion,

performed for isotropic spectrum, which is given and discussed in the supporting information (Figures S3–S8).

Refinement with the Cartesian coordinates of Mn2 and Mn3 fixed

Interestingly, although the refined cluster model reproduces the experimental spectra well, it does not contain any O-bridged Mn–Mn distance as long as 3.2–3.4 Å as in all OEC models suggested by EXAFS (Figure 3) and also in the latest XRD structure (3.3 Å);[4] the longest such Mn–Mn distance in the refined cluster model is 3.11 Å. To test the possibility of one longer Mn–Mn vector in the topology of the cluster model, the Cartesian coordinates of Mn2 and Mn3 (labeled as in Figure 3) were fixed at a distance of 3.2 Å during the QM/pEXAFS refinement. Figure 4 compares the spectra calculated after the constrained refinement with the experimental data. A qualitative consistency is clearly achieved with χ^2 = 61 (Table 1). Therefore, both the refined and the constrained refined models are reasonable local solutions relative to the QM minima, and a discrimination between the two models cannot be made in the current theoretical EXAFS study. It is conceivable that the longer Mn–Mn distance in both the XRD and EXAFS structures is caused by partial photoreduction of the sample during data collection (note that all XRD Mn–Mn distances are 0.1–0.4 Å longer than in the cluster model, cf. Figure 3, as can be expected if the metal ions are reduced).
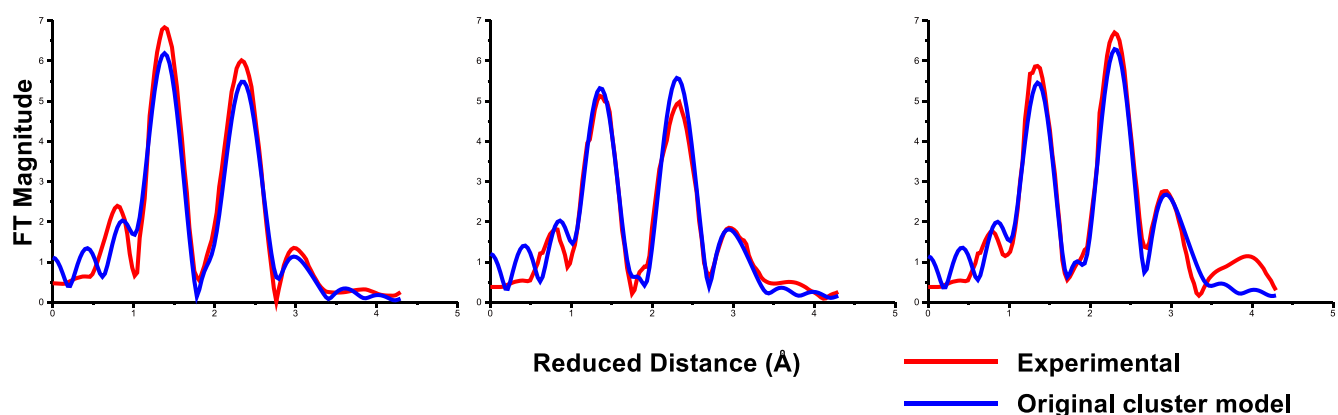

FIGURE 4. Comparison of the experimental polarized EXAFS spectra (red), along the PSII crystal axes *a*, *b*, and *c*, and the calculated spectra (blue) for the refined cluster model with the Cartesian coordinates of Mn2 and Mn3 fixed with a Mn2–Mn3 distance of 3.2 Å.

CONCLUSIONS

In summary, we have developed a method to combine QM geometry optimizations with a polarized EXAFS fit. Such an approach is appreciably more accurate than previous approaches,[10,11] which only use a simple geometric harmonic restraints to a QM/MM structure. In particular, we ensure that the final structure is an optimum compromise between the QM and EXAFS data, that the induced changes in the structure is chemically reasonable and affect only

the part of the structure that is most flexible. Moreover, we can quantify the change in structure in energy terms.

The results show that the QM cluster model of the OEC in PSII can qualitatively reproduce the experimental polarized EXAFS spectra with only slight structural distortions, which provides a significant additional piece of evidence for the adequacy of this model. Thus, no surrounding enzyme is needed to reproduce the EXAFS data. Moreover, the QM structures have well-defined oxidation states of the Mn ions, avoiding the problem of partial photoreduction, which strongly affects XRD structures. However, it is important to note that several topologically different structures fit polarized EXAFS equally well. Our results also show that structures with no bridged Mn–Mn distance larger than 3.1 Å fit the experimental polarized EXAFS data as well as a structure with a single Mn–Mn bond of 3.2 Å. This does not necessarily mean that the structure lacks a long Mn–Mn distance, but it shows that it is at present not possible to use polarized EXAFS alone to determine whether there is a longer bond or not.

ACKNOWLEDGEMENTS

Supporting Information Available. Cartesian coordinates of the refined cluster model. Figures of the calculated polarized EXAFS spectra in *k*-space, a comparison of the experimental and the calculated polarized EXAFS spectra with certain atoms removed, a comparison of calculated isotropic EXAFS spectrum, the individual atomic contributions to whole isotropic spectrum, the and scattering contributions to the isotropic EXAFS spectra of the Mn ions based on path analysis.

REFERENCES AND NOTES

1.   Ferreira, K. N.; Iverson, T. M.; Maghlaoui, K.; Barber, J.; Iwata, S., Architecture of the Photosynthetic Oxygen-Evolving Center. *Science* **2004,** *303* (5665), 1831-1838.
2.   Loll, B.; Kern, J.; Saenger, W.; Zouni, A.; Biesiadka, J., Towards complete cofactor arrangement in the 3.0[thinsp]A resolution structure of photosystem II. *Nature* **2005,** *438* (7070), 1040-1044.
3.   Guskov, A.; Kern, J.; Gabdulkhakov, A.; Broser, M.; Zouni, A.; Saenger, W., Cyanobacterial photosystem II at 2.9-A resolution and the role of quinones, lipids, channels and chloride. *Nat Struct Mol Biol* **2009,** *16* (3), 334-342.
4.   Umena, Y.; Kawakami, K.; Shen, J.-R.; Kamiya, N., Crystal structure of oxygen-evolving photosystem II at a resolution of 1.9 Å. *Nature* **2011,** *473* (7345), 55-60.

5.   Yano, J.; Kern, J.; Sauer, K.; Latimer, M. J.; Pushkar, Y.; Biesiadka, J.; Loll, B.; Saenger, W.; Messinger, J.; Zouni, A.; Yachandra, V. K., Where Water Is Oxidized to Dioxygen: Structure of the Photosynthetic Mn4Ca Cluster. *Science* **2006,** *314* (5800), 821-825.

6.   Zein, S.; Kulik, L. V.; Yano, J.; Kern, J.; Pushkar, Y.; Zouni, A.; Yachandra, V. K.; Lubitz, W.; Neese, F.; Messinger, J., Focusing the view on nature's water-splitting catalyst. *Philosophical Transactions of the Royal Society B: Biological Sciences* **2008,** *363* (1494), 1167-1177.

7.   Pantazis, D. A.; Orio, M.; Petrenko, T.; Zein, S.; Lubitz, W.; Messinger, J.; Neese, F., Structure of the oxygen-evolving complex of photosystem II: information on the S_2 state through quantum chemical calculation of its magnetic properties. *PCCP* **2009,** *11*, 6788-6798.

8.   Barber, J.; Murray, J. W., The structure of the Mn4Ca2+ cluster of photosystem II and its protein environment as revealed by X-ray crystallography. *Philosophical Transactions of the Royal Society B: Biological Sciences* **2008,** *363* (1494), 1129-1138.

9.   Sproviero, E. M.; Gascón, J. A.; McEvoy, J. P.; Brudvig, G. W.; Batista, V. S., QM/MM Models of the O2-Evolving Complex of Photosystem II. *Journal of Chemical Theory and Computation* **2006,** *2* (4), 1119-1134.

10.   Sproviero, E. M.; Gascón, J. A.; McEvoy, J. P.; Brudvig, G. W.; Batista, V. S., A Model of the Oxygen-Evolving Center of Photosystem II Predicted by Structural Refinement Based on EXAFS Simulations. *J. Am. Chem. Soc.* **2008,** *130* (21), 6728-6730.

11.   Luber, S.; Rivalta, I.; Umena, Y.; Kawakami, K.; Shen, J.-R.; Kamiya, N.; Brudvig, G. W.; Batista, V. S., S1-State Model of the O2-Evolving Complex of Photosystem II. *Biochemistry* **2011,** *50* (29), 6308-6311.

12.   Siegbahn, P. E. M., O-O Bond Formation in the S_4 State of the Oxygen-Evolving Complex in Photosystem II. *Chemistry - A European Journal* **2006,** *12* (36), 9217-9227.

13.   Siegbahn, P. E. M., A Structure-Consistent Mechanism for Dioxygen Formation in Photosystem II. *Chemistry - A European Journal* **2008,** *14* (27), 8290-8302.

14.   Siegbahn, P. E. M., Structures and Energetics for O2 Formation in Photosystem II. *Acc. Chem. Res.* **2009,** *42* (12), 1871-1880.

15.   Siegbahn, P. E. M., Water oxidation in photosystem II: oxygen release, proton release and the effect of chloride. *Dalton Transactions* **2009,** (45), 10063-10068.

16.   Siegbahn, P. E. M., An Energetic Comparison of Different Models for the Oxygen Evolving Complex of Photosystem II. *J. Am. Chem. Soc.* **2009,** *131* (51), 18238-18239.

17.   Siegbahn, P. E. M., The Effect of Backbone Constraints: The Case of Water Oxidation by the Oxygen-Evolving Complex in PSII. *ChemPhysChem* **2011,** *12* (17), 3274-3280.

18.   Hsiao, Y.-W.; Tao, Y.; Shokes, J. E.; Scott, R. A.; Ryde, U., EXAFS structure refinement supplemented by computational chemistry. *Physical Review B* **2006,** *74* (21), 214101.

19.   Ryde, U.; Hsiao, Y.-W.; Rulíšek, L.; Solomon, E. I., Identification of the Peroxy Adduct in Multicopper Oxidases by a Combination of Computational Chemistry and Extended X-ray Absorption Fine-Structure Measurements. *J. Am. Chem. Soc.* **2007,** *129* (4), 726-727.

20.   Ankudinov, A. L.; Ravel, B.; Rehr, J. J.; Conradson, S. D., Real-space multiple-scattering calculation and interpretation of x-ray-absorption near-edge structure. *Physical Review B* **1998,** *58* (12), 7565-7576.

21.   Ankudinov, A. L.; Bouldin, C. E.; Rehr, J. J.; Sims, J.; Hung, H., Parallel calculation of electron multiple scattering using Lanczos algorithms. *Physical Review B* **2002,** *65* (10), 104107.

22.   Newville, M., IFEFFIT : interactive XAFS analysis and FEFF fitting. *Journal of Synchrotron Radiation* **2001,** *8* (2), 322-324.

23.   Ryde, U.; Olsen, L.; Nilsson, K., Quantum chemical geometry optimizations in proteins using crystallographic raw data. *J. Comput. Chem.* **2002,** *23* (11), 1058-1070.

24.   Hsiao, Y.-W.; Drakenberg, T.; Ryde, U., NMR structure determination of proteins supplemented by quantum chemical calculations: Detailed structure of the Ca<sup>2+</sup> sites in the EGF34 fragment of protein S. *J. Biomol. NMR* **2005,** *31* (2), 97-114.

25.   Kleywegt, G. J.; Alwyn Jones, T., [11] Model building and refinement practice. In *Methods Enzymol.*, Charles W. Carter Jr, R. M. S., Ed. Academic Press: 1997; Vol. Volume 277, pp 208-230.

26.   Cavanagh, J.; Fairbrother, W. J.; Palmer, A. G.; Skelton, N. J., *Protein NMR Spectroscopy: Principles and Practice*. Academic Press: London, 1996.

27.   Ahlrichs, R.; Bär, M.; Häser, M.; Horn, H.; Kölmel, C., Electronic structure calculations on workstation computers: The program system turbomole. *Chem. Phys. Lett.* **1989,** *162* (3), 165-169.

28.   Eichkorn, K.; Treutler, O.; Öhm, H.; Häser, M.; Ahlrichs, R., Auxiliary basis sets to approximate Coulomb potentials. *Chem. Phys. Lett.* **1995,** *240* (4), 283-289.

29.   Treutler, O.; Ahlrichs, R., Efficient molecular numerical integration schemes. *The Journal of Chemical Physics* **1995,** *102* (1), 346-354.

30.   Eichkorn, K.; Weigend, F.; Treutler, O.; Ahlrichs, R., Auxiliary basis sets for main row atoms and transition metals and their use to approximate Coulomb potentials. *Theoretical Chemistry Accounts: Theory, Computation, and Modeling (Theoretica Chimica Acta)* **1997,** *97* (1), 119-124.

31.   Von Arnim, M.; Ahlrichs, R., Performance of parallel TURBOMOLE for density functional calculations. *J. Comput. Chem.* **1998,** *19* (15), 1746-1757.

32.   Weigend, F.; Ahlrichs, R., Balanced basis sets of split valence, triple zeta valence and quadruple zeta valence quality for H to Rn: Design and assessment of accuracy. *PCCP* **2005,** *7*, 3297-3305.

33.   Weigend, F., Accurate Coulomb-fitting basis sets for H to Rn. *PCCP* **2006,** *8* (9), 1057-1065.

34.   Penner-Hahn, J. E., X-ray absorption spectroscopy in coordination chemistry. *Coord. Chem. Rev.* **1999,** *190-192*, 1101-1123.

35.   Sigfridsson, E.; Olsson, M. H. M.; Ryde, U., A Comparison of the Inner-Sphere Reorganization Energies of Cytochromes, Iron–Sulfur Clusters, and Blue Copper Proteins. *The Journal of Physical Chemistry B* **2001,** *105* (23), 5546-5552.

36.   Ryde, U.; Nilsson, K., Quantum Chemistry Can Locally Improve Protein Crystal Structures. *J. Am. Chem. Soc.* **2003,** *125* (47), 14232-14233.

37.   Siegbahn, P. E. M., O-O bond cleavage and alkane hydroxylation in methane monooxygenase. *J. Biol. Inorg. Chem.* **2001,** *6* (1), 27-45.